

25 **Code availability**

26 The R package demres is freely available on GitHub:

27 <https://github.com/JulieLouvrier/demres>. We also intend to submit it to CRAN.

28 **Data availability**

29 The data attached with the package can be found in the package repository in Github, or by
30 calling `data(bluecrane)` after loading the package.

31

32 **Conflict of interest**

33 The authors declare no conflict of interest.

34

35 **Acknowledgements**

36 We thank Oliver Höner from the WILDER project for his critical comments on the
37 manuscript., JL, EWW, ATC, SB and VR acknowledge BMBF project WILDER (Number
38 16DKWN148) for financial support.

39

40 **Authors contributions**

41 JL conceptualization, package development, writing, AC package development, writing,
42 EWW package development, writing, ATC conceptualization, writing, SB conceptualization,
43 writing, VR conceptualization, package development, writing.

44 **Abstract**

45 1- Quantifying the resilience of populations to disturbances is essential to assess how
46 threatened populations are. Demographic resilience has been defined as the ability of
47 populations to resist and recover from alterations in their demographic structures. Resilience
48 metrics are typically obtained by applying transient analyses to matrix population models.
49 Until now, the questions of how demographic resilience can change over time, how to
50 quantify such temporal variation and when it is important to account for it have not yet been
51 studied. However, since demographic rates fluctuate over time, it is essential to evaluate
52 whether and under what conditions the assumption of time-constant demographic resilience
53 remains appropriate.

54 2- In this study we introduce demres - an R package that offers functions to quantify time-
55 varying and time-constant demographic resilience metrics, including time to convergence,
56 damping ratio, inertia, maximum amplification, maximum attenuation and reactivity. The
57 package also allows the comparison of these two approaches, both visually and by means of
58 distance metrics.

59 3- We use a case study to illustrate the versatility of demres and demonstrate how this tool
60 can be readily used by conservation biologists, managers and others to assess the time-
61 varying resilience of wildlife populations using long-term demographic data. Our framework
62 facilitates standardised comparisons of demographic resilience metrics, for example by
63 means of comparative studies across populations and species.

64

65 **Keywords**

66 Demographic resilience, amplification, resistance, transient analyses, matrix population
67 models, R package, disturbance

68 **Introduction**

69 Quantifying resilience is essential to predict the fate of populations living in environments
70 that are undergoing change. Capdevila et al. (2020) defined demographic resilience as the
71 ability of populations to resist and recover from alterations in their demographic structures.
72 By measuring demographic resilience we can assess immediate, short-term, response of
73 populations to disturbances, which proved useful when assessing for example the influence of
74 environmental stochasticity on populations (Gilbert et al., 2020). Demographic resilience
75 metrics are quantified by applying matrix population models (MPMs, Caswell, 2006) analyse
76 the short-term (i.e. transient) response of populations to disturbances (Stott et al., 2011,
77 2012). As input, MPMs use vital rates that summarise the survival and fecundity of age or
78 stage classes of the population. The common approach to quantify demographic resilience
79 when vital rates have been collected over a certain period of time is to average them over that
80 period and to use a so-called time-averaged matrix (Capdevila et al., 2020, 2021). This
81 approach is generally common practice in classical demographic analyses of MPMs that
82 focus on long-term (i.e. asymptotic) population dynamics (Caswell, 2006). In the case of
83 transient analysis that focuses on short-term dynamics, the averaging of vital rates over time
84 implicitly assumes that they do not vary strongly enough in time to warrant quantification of
85 temporally-varying demographic resilience. However, it is unclear whether this assumption is
86 justified. As vital rates are reported to vary strongly over time across species and study
87 systems (Bailey et al., 2024; Jenouvrier et al., 2022; Jonzén et al., 2010; Marescot et al.,
88 2018) so are demographic resilience metrics likely to vary over time too.

89 Long-term studies of populations in the wild show that vital rates can vary strongly
90 over time (Bailey et al., 2024; Jenouvrier et al., 2022; Jonzén et al., 2010; Marescot et al.,
91 2018), either due to abiotic natural environmental variability, biotic inter- and intraspecific
92 interactions or due to anthropogenic disturbances (e.g. climate change or poaching). For

93 example, the survival of cubs and subadults of spotted hyenas (*Crocuta crocuta*) in the
94 Serengeti National Park declined strongly in response to a canine distemper virus outbreak in
95 1993/1994 (Benhaïem et al., 2018). Hunting, by targeting specific age classes, may disrupt
96 the demographic structures of populations, leading to transient dynamics (Koons et al., 2005).
97 For instance, the survival of black rhinoceros *Diceros bicornis* in north-West Namibia has
98 increased after protection from illegal poaching (Brodie et al., 2011). As vital rates vary in
99 time, the resulting demographic resilience is also expected to vary in time. However, the
100 extent of such variation, when to account for it and the conditions that cause extreme
101 fluctuations over time remain unknown. In a world where disturbances are on the rise
102 (Turner, 2010), gaining a better understanding of the variations in the short-term responses to
103 these disturbances can be crucial for conservation, wildlife management (Gerber & Kendall,
104 2016).

105 Here we propose the R package demres, which provides functions to quantify time-
106 varying and time-constant demographic resilience, as well as to compare these two
107 approaches both visually and by means of several distance metrics. We expect that demres
108 will motivate quantification of time-varying demographic resilience for populations where
109 relevant data is available. This, in turn, will facilitate comparative cross-study analyses that
110 would ultimately assess for what species or populations and under what environmental
111 conditions the assumption of time-constant demographic resilience holds.

112 **How to assess demographic resilience**

113 Analyses of demographic resilience come from the framework of transient analyses (Caswell,
114 2006; Stott et al., 2011). This approach relies on (i) a matrix denoted \mathbf{A} summarising the vital
115 rates of the population and (ii) an initial demographic distribution representing the initial
116 abundance distribution of each age or stage class of the study population; hereafter referred to
117 as “(st)age” class for short. These two elements are thus key inputs that the user must provide

118 to demres. Finally, using these two elements, the population is projected and its transient
119 behaviour is quantified before it reaches asymptotic growth. These transient analyses allow
120 calculating a set of demographic resilience metrics including convergence time, damping
121 ratio, inertia, maximum amplification, maximum attenuation and reactivity (Table 1).

122 **Matrix Population Models**

123 In the fields of ecology and conservation biology, MPMs have become the most widespread
124 tool to forecast population dynamics. The MPM is a mathematical representation of the
125 change of distribution of individuals across different stages (e.g. size, or developmental
126 stage) or age classes in a population over time (Caswell, 2006). The MPMs are built around a
127 matrix **A** where the elements (known as vital rates) define, per unit of time, survival rates in a
128 given (st)age, transition probabilities from one (st)age to another, and fecundity (i.e. per-
129 capita number of offspring that is contributed to the population by each (st)age).

130 **Demographic distribution**

131 The initial demographic distribution represents the abundance of individuals in each (st)age
132 class by a vector (\hat{n}_0). Such demographic distributions can be obtained from: i) a known
133 (st)age-class distribution that is representative of the population being studied; or ii) stage-
134 biased vectors that represent the most extreme cases where only one (st)age class is
135 represented in the population, whereas abundances of all others are set to “0” (Townley &
136 Hodgson, 2008).

137 Since demographic distribution often is not available for wild-living species, most
138 existing studies apply option ii) to study resilience. Using stage-biased vectors provides the
139 extreme plausible population responses to a disturbance, which are called the transient
140 bounds (Stott et al., 2011; Townley & Hodgson, 2008). These bounds delineate the range of
141 responses that a population can exhibit. Since stage-biased vectors are biased towards one

142 (st)age class, there are as many stage-biased vectors as there are classes. For example, a
143 population with four (st)age classes will have the four following standardised stage-biased
144 vectors: [1 0 0 0]; [0 1 0 0]; [0 0 1 0]; [0 0 0 1]. The stage-biased vectors are automatically
145 computed by demres, thus facilitating the transient analyses, especially if many (st)ages are
146 distinguished.

147 **Standardising MPMs and vectors**

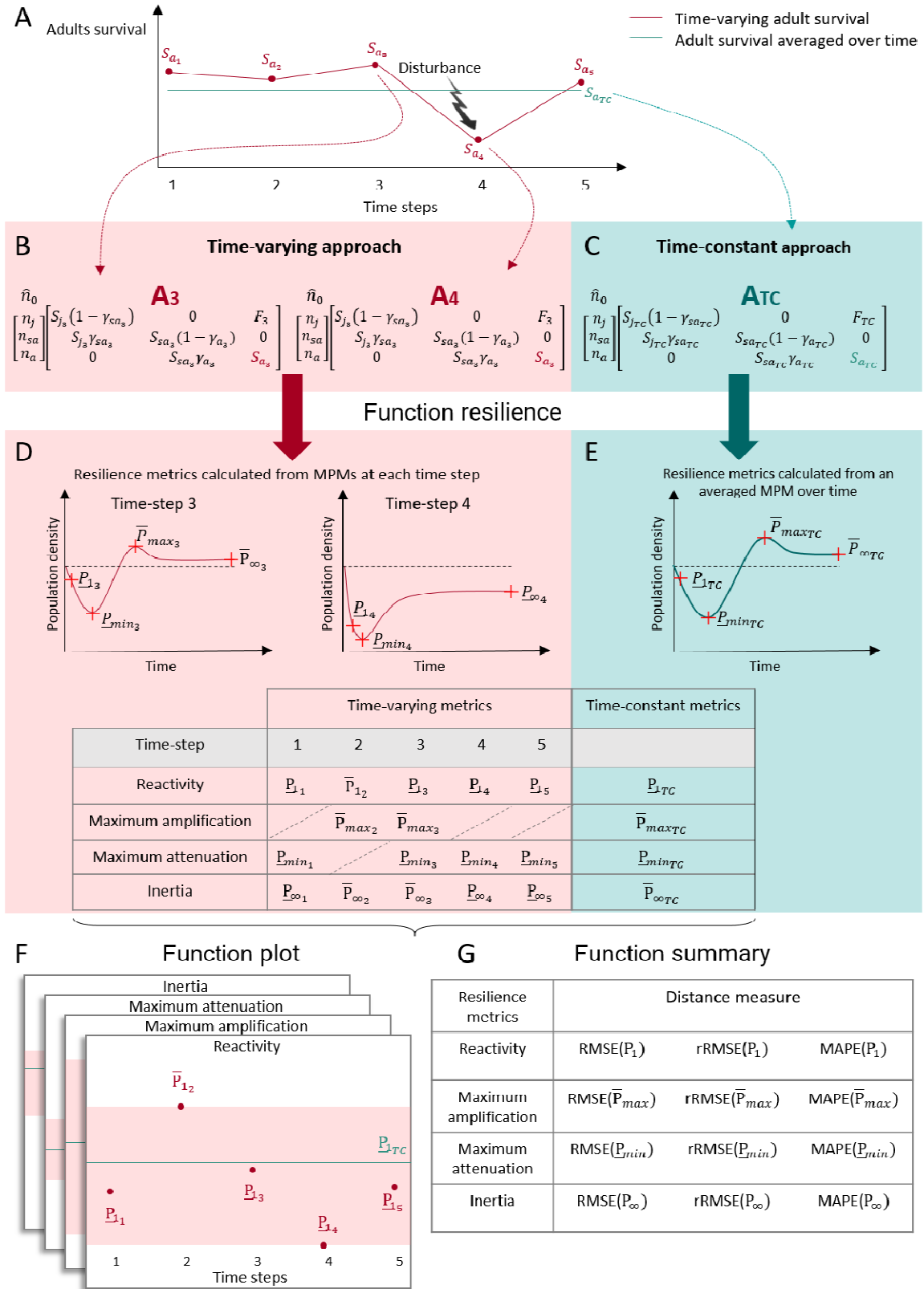
148 Transient analyses can be performed in two ways (Stott et al., 2011). The first option uses
149 absolute change in population abundance and thus describes the combined influence of both
150 transient and asymptotic dynamics. The second option uses relative measures of transient
151 dynamics, which allows disentangling the transient and asymptotic effects and therefore
152 enables the comparison of populations with very different ranges of transient dynamics (Stott
153 et al., 2011). For this, the matrix \mathbf{A} is divided by λ_{max} , the asymptotic growth rate, and the
154 initial vector is divided by the total sum of individuals to get a total population density of 1.
155 The package demres uses the matrices that are divided by λ_{max} , but the users can decide to
156 provide absolute or relative vectors.

157 **Comparison of the time-varying and the time-constant approaches**

158 When data is collected from multiple years, or other biologically relevant time-steps, vital
159 rates are calculated and matrices can therefore be built for each of these time-steps (Fig. 1A).
160 Time-step for MPMs should be chosen so as to best reflect the life cycle of a study species
161 (Enright et al., 1995). The time-varying approach considers vital rates calculated at each
162 time-step (Fig. 1A). A matrix summarising these vital rates is then constructed for each of
163 these time-steps and the transient analysis is performed on each of these matrices (Fig. 1B),
164 providing resilience metrics at each time-step (Fig. 1D). In contrast, the time-constant
165 approach relies on a matrix that is averaged over time (Fig. 1C) and thus returns only one

166 value for each demographic resilience metric over the whole study period (Fig. 1E). For
167 example, if a population was monitored for ten years and a time-step was a year, each of the
168 demographic resilience metrics will be computed ten times following the time-varying
169 approach, and once following the time-constant approach. Importantly, the average of the
170 resilience metrics obtained with the time-varying approach is usually not equal to the
171 resilience metric derived from the averaged population matrix (i.e. time-constant approach).
172 The package demres allows for a visual comparison of the metric values obtained with the
173 time-constant and time-varying approaches (Fig. 1F). To assess to what extent the
174 demographic resilience metrics vary over time, demres computes the distance between the
175 single value returned for the whole time series by the time-constant approach and all the
176 time-specific values from the time-varying approach (Fig. 1G). Three distances can be
177 computed: residual mean squared error (RMSE), relative residual mean squared error
178 (rRMSE) and the mean absolute proportional error (MAPE, see demres vignette for formulas)
179 (Hodson, 2022).

180



181

182

183 Figure 1: The workflow of the demres package. (A) In a hypothetical population with three
184 stage classes; juveniles, subadults and adults, the vital rates vary over time. Here we display
185 the survival of adults (S_a), which is negatively affected by the disturbance that happens in the
186 fourth year of the study. (B) The time-varying approach considers a matrix A_x for each time-
187 step x and an initial demographic distribution \hat{n}_0 and calculates the demographic resilience
188 metrics at each time-step, capturing the temporal variation in vital rates. The index x indicates
189 the time-step. The elements of the matrix A_x are: S_{j_x} , S_{sa_x} , and S_{a_x} - survival of juveniles,
190 subadults and adults, respectively; and F_x - fecundity. γ_{sa_x} and γ_{a_x} are the transition
191 probabilities from juvenile to subadult and from subadult to adult, respectively. In \hat{n}_0 , n_j , n_{sa}
192 and n_a represent the relative proportion of juveniles, subadults and adults in the population.
193 (C) The time-constant approach uses an averaged matrix A_{TC} that is obtained by averaging
194 over the annual vital rate values. The index TC indicates the time-constant approach. (D)
195 Given the initial population distribution and the matrix A_x , the demographic resilience
196 metrics are calculated, e.g. reactivity, maximum attenuation and inertia (see Table 1 for
197 formulas). Following Stott et al. 2011, we used the Latin P to represent demographic
198 resilience metrics calculated with a specific initial demographic distribution \hat{n}_0 (in opposition
199 to the Greek ρ used to represent the bounds, see appendix 1 for the formulas of the bounds).
200 An overbar ($\bar{}$) indicates an index of amplification, whereas an underbar ($\underline{}$) represents an
201 index of attenuation. The direction of the metrics have been chosen for illustration purposes
202 only in this example. It is possible that the population does not amplify, as is the case here for
203 the time-steps one, four and five. The population also did not attenuate when using the matrix
204 \square_2 for the time-step two. (E) Under the time-constant approach the population attenuated and
205 amplified. The package demres also provides: (F) a plot function visualising the resulting
206 demographic resilience metrics, and (G) a summary function providing measures of distance
207 between the time-varying and the time-constant metrics. The symbols shown in orange/blue
208 denote, respectively, the metrics calculated under time-varying and time-constant approach.
209

210 Resilience metrics

211 Demographic resilience is commonly quantified with a set of resilience metrics (Table 1,
212 Capdevila et al. 2020, Stott et al. 2011). The main goal of demres is to compute them using
213 either a time-varying or time-constant approach, or both.

214 Table 1: resilience metrics provided by demres, their calculation and interpretation. **A**
 215 is the population matrix. $\hat{\mathbf{A}}$ is the standardised matrix, which is calculated as \mathbf{A}/λ_{max} , where
 216 λ_{max} is the dominant eigenvalue of **A**. w is the dominant right eigenvector and the stable
 217 demographic structure of **A**. v represents the dominant left eigenvector, the reproductive
 218 value vector of **A**. The vector \hat{n}_0 represents the initial demographic distribution, standardised
 219 to sum to 1. $\|m\|_1$ is the one-norm of a vector m (equal to the sum of the entries for m).
 220 Following Stott et al. 2011, the case-specific demographic resilience metrics (i.e. calculated
 221 with a specific initial demographic distribution \hat{n}_0) are represented with the Latin P (See
 222 appendix 1 for a similar table done for the bounds). An overbar ($\bar{}$) indicates an index of
 223 amplification, whereas an underbar ($\underline{}$) represents an index of attenuation. Transient metric
 224 subscripts provide information regarding the timeframe of a study, where 1 indicates first
 225 time-step; *max* and *min* are maximum amplification and attenuation, respectively, and ∞
 226 is inertia. λ_1 is the dominant eigenvalue, λ_2 is the largest subdominant eigenvalue. Formulas,
 227 descriptions and table structure are based on Table 1 of Capdevila et al. (2020) and Stott et al.
 228 (2011). Interpretation of all metrics except convergence time and damping ratio are to be
 229 made relative to a population with stable growth rate.
 230

Resilience Component	Metric	Name in demres	Calculation	Interpretation
Recovery	Convergence time	“convt”	Works by projecting the population forward until convergence to the given accuracy is reached	Time to convergence of a population matrix projection model from the model projection.
	Damping ratio	“dr”	$\rho = \frac{\lambda_1}{\ \lambda_2\ }$	Dimensionless measure of convergence to stable growth. Smaller numbers represent slower

				convergence.
Amplification	Inertia	“inertia”	$\bar{P}_\infty = \frac{v^T \hat{n}_0 \ w\ _1}{v^T w}$ when $\frac{v^T \hat{n}_0 \ w\ _1}{v^T w} > 1$	The long-term population density of a given population
	Maximum amplification	“maxamp”	$\bar{P}_{max} = \max_{t>0} (\hat{A}^t \hat{n}_0)$ when $ \hat{A}^t \hat{n}_0 > 1$ for some t	The largest possible reachable population density
	Reactivity	“reac”	$\bar{P}_1 = \ \hat{A} \hat{n}_0\ _1$ when $\ \hat{A} \hat{n}_0\ _1 > 1$	The population density reached in the first time-step
Resistance	Inertia	“inertia”	$\underline{P}_\infty = \frac{v^T \hat{n}_0 \ w\ _1}{v^T w}$ when $\frac{v^T \hat{n}_0 \ w\ _1}{v^T w} < 1$	The long-term population density of a given population
	Maximum attenuation	“maxatt”	$\underline{P}_{min} = \max_{t>0} (\hat{A}^t \hat{n}_0)$ when $ \hat{A}^t \hat{n}_0 < 1$ for some t	The smallest possible reachable population density
	Reactivity	“reac”	$\underline{P}_1 = \ \hat{A} \hat{n}_0\ _1$ when $\ \hat{A} \hat{n}_0\ _1 < 1$	The population density reached in the first time-step

232

233 **Package overview**

234 The package demres will be available on GitHub: [true link will be added during proof] and
235 will be submitted to CRAN. It is inspired and based on the popdemo package (Stott et al.,
236 2012). The main function in demres is called resilience. We also programmed methods for
237 the generic functions summary and plot working with the outputs produced by resilience.
238 When designing demres we decided to follow the same syntax as in popdemo so as to
239 facilitate an easy transition between the packages for the users.

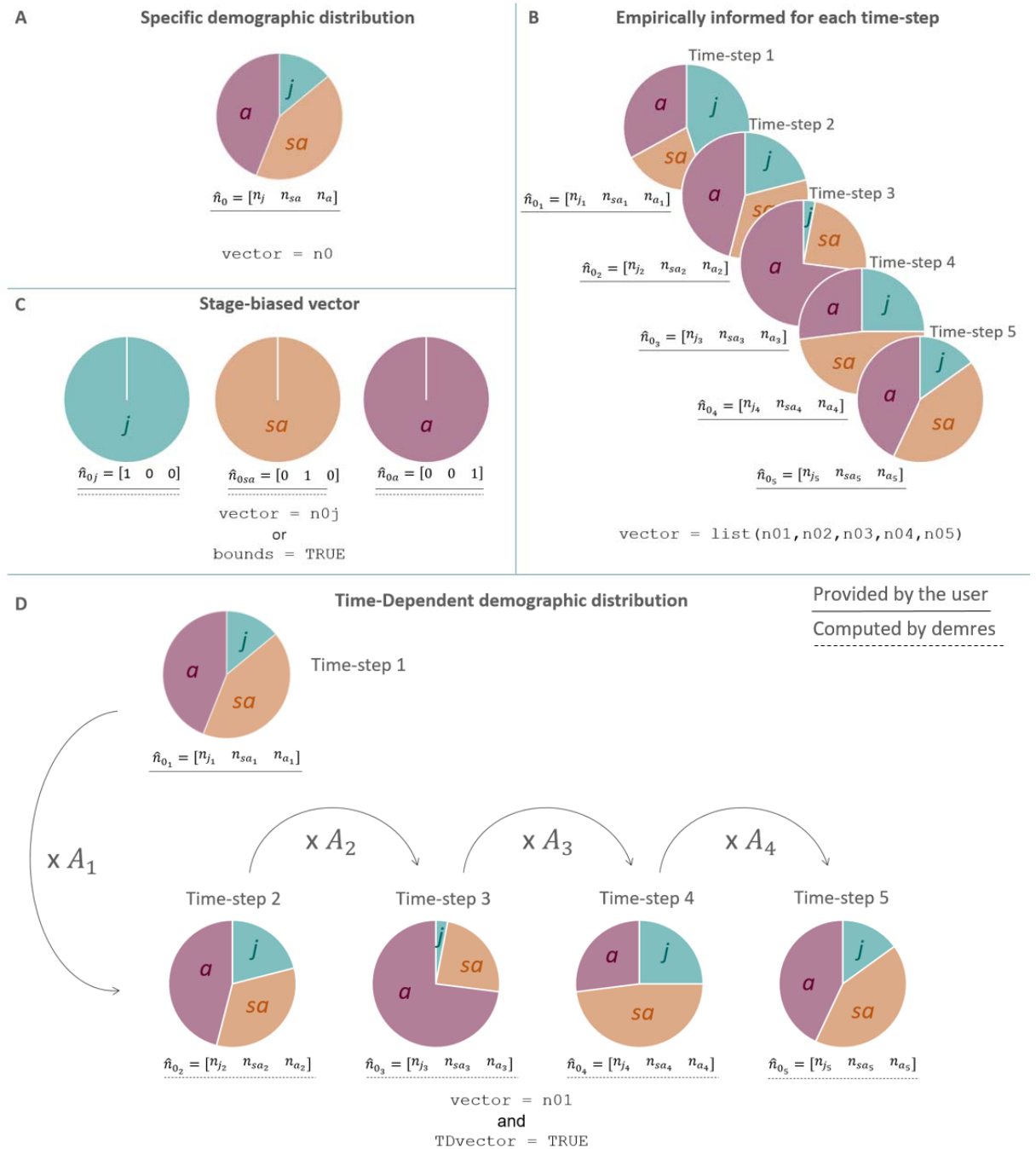
240 **Calculate demographic resilience metrics based on a list of Matrix Population**

241 **Models**

242 The core function resilience allows calculating demographic resilience metrics using a list of
243 matrices computed at each time-step of the study. The user can choose to compute a specific
244 metric, several metrics, or all available metrics, including convergence time ("convt"),
245 damping ratio ("dr"), inertia ("inertia"), maximum amplification ("maxamp"), maximum
246 attenuation ("maxatt") and reactivity ("reac", Table 1). The choice of which metrics to use is
247 done by setting the argument metrics. The user can choose to compute the metrics using
248 either time-varying, time-constant or both approaches, using the argument time.

249 The initial demographic distribution can be specified in several ways, depending on
250 the main goal of the analyses and the data availability. If the focus is on dynamics of a
251 population with a particular demographic distribution (e.g. in reintroduction scenarios), then
252 (i) this distribution can be supplied as one vector in vector (Fig. 2 A). If the goal is to assess
253 resilience of the studied population over a certain time period in the past and demographic
254 distribution for each time-step is available, the user can (ii) supply a list of vectors of (st)age-
255 class distributions for each time-step in vector (Fig. 2 B). In cases when the interest lies in

256 comparing resilience metrics across studies, the user can (iii) request bounds to be calculated
257 from the (st)age-biased vectors by using `bounds = TRUE` or supplying manually one stage-
258 biased vector in `vector` (Fig. 2 C). Finally, if the goal is, similarly to the option (ii) to assess
259 resilience of a population in the past but not enough detailed data is available to extract
260 demographic distribution for each time-step, then (iv) a population can be projected from a
261 given initial demographic distribution and a list of matrices over a certain time period, using
262 `TDvector = TRUE` for Time-Dependent vector. The demographic distribution for the
263 following time step is then projected based on the provided initial demographic distribution
264 and the respective matrix for that time-step. This procedure reiterates across all time-steps
265 (Fig. 2 D).



266

267 Figure 2: Representation of the different options a user has when specifying the demographic
 268 distribution when studying a population structured in three stage classes juveniles, subadult
 269 and adults. (A) In the case of assessing the demographic resilience of a population with a
 270 specific abundance of juveniles (represented as j), subadults (sa) and adults (a), then the user
 271 can provide in vector with \hat{n}_0 , the relative density of juveniles, subadults and
 272 adults in the population, respectively. (B) In the case where the demographic distribution is

273 known for each time-step, then the user can provide a list of vectors \hat{n}_{0_x} for each time-step x
274 in vector. (C) In the case of assessing the transient bounds, the user can either provide the
275 stage-biased vector and test for each one of them or use the argument `bounds` specified to
276 return the bounds of each of the resilience metrics. Finally, if a specific demographic
277 structure is known but then needs to be projected over each time-step, then the user can
278 provide \hat{n}_0 in vector for the first time-step and use the argument `TDvector` for demres to
279 compute the initial vectors for the rest of the time-steps.

280

281 **Case study**

282 **Description of the blue crane study**

283 The data distributed with this package (`bluecrane`) comes from a study by (Altwegg &
284 Anderson, 2009) of a blue crane population (*Anthropoides paradiseus*) in South Africa. This
285 population was monitored between 1997 and 2008, with a total of 451 individuals ringed to
286 assess how rainfall impacted vital rates. Five age classes were distinguished. The study
287 revealed that the survival of blue cranes in all age classes increased with increasing rainfall in
288 the late breeding season, and varied substantially over the 12 years of the study, with lowest
289 values in the fifth year and highest values in the second year of the study. The reproductive
290 output of blue cranes also varied substantially over time, being higher in the years with higher
291 rainfall during the early breeding season. As a result, we expected demographic resilience to
292 vary with time.

293 **Assess demographic resilience metrics**

294 We extracted the 12 MPMs for each time-step of the study from the COMADRE database
295 (Salguero-Gómez et al., 2016). COMADRE contains MPMs of animal species, which can be
296 directly downloaded from their website (<https://compadre-db.org/>) or using the R package
297 `Rcompadre` (Jones et al., 2022).

298 For illustration purposes, we here focus on quantifying a single resilience metric: reactivity.
299 Since this species is vulnerable (IUCN 2024) and reproduction can be lowered due to climate,
300 we use an initial demographic distribution with an under-representation of the first age class.
301 The function `resilience` is used to specify the list of matrices with the argument `listA` and the
302 metric to be calculated ("`reac`") with the argument `metrics`. If the user wants to compute the
303 bounds, then the argument `bounds` should be set to `TRUE`. Finally, if the metric is to be
304 calculated using both time-varying and time-constant approaches then `time` should be set to
305 "`both`":

```
n0 <- c(0.04, 0.22, 0.22, 0.22, 0.30)
BC_reac <- resilience(
  listA = bluecrane,
  metrics = "reac",
  bounds = TRUE,
  vector = n0,
  popname = "blue crane",
  time = "both")
```

306 The time-constant reactivity obtained is 1.31 (Table 2) with the lower bound at a value of
307 0.53 and the upper bound at a value of 2.90. A reactivity of 1.31 means that as the immediate
308 response to a disturbance the population will grow 1.31 times faster than its stable growth
309 rate. The time-varying reactivity varies between 1.22 (time-step 5) and 1.44 (time-step 2)
310 when calculated with the supplied initial vector. The lower bound varies between 0.49 (time-
311 step 5) and 0.57 (time-step 2) while the upper bound varies between 2.52 (time-step 5) and
312 3.38 (time-step 2). The time-varying reactivity differs most from the time-constant value
313 when using the upper bound (Fig. 3). This conclusion is also supported by RMSE and MAPE,
314 whose values are largest when calculated at the upper bound (Table 3).

315 Table 2: Reactivity of the blue crane population calculated using both approaches (time-
316 varying: TV, time-constant: TC). Values that were calculated using the initial demographic
317 distribution are shown as `reac`, and those calculated using the (st)age-biased vectors are

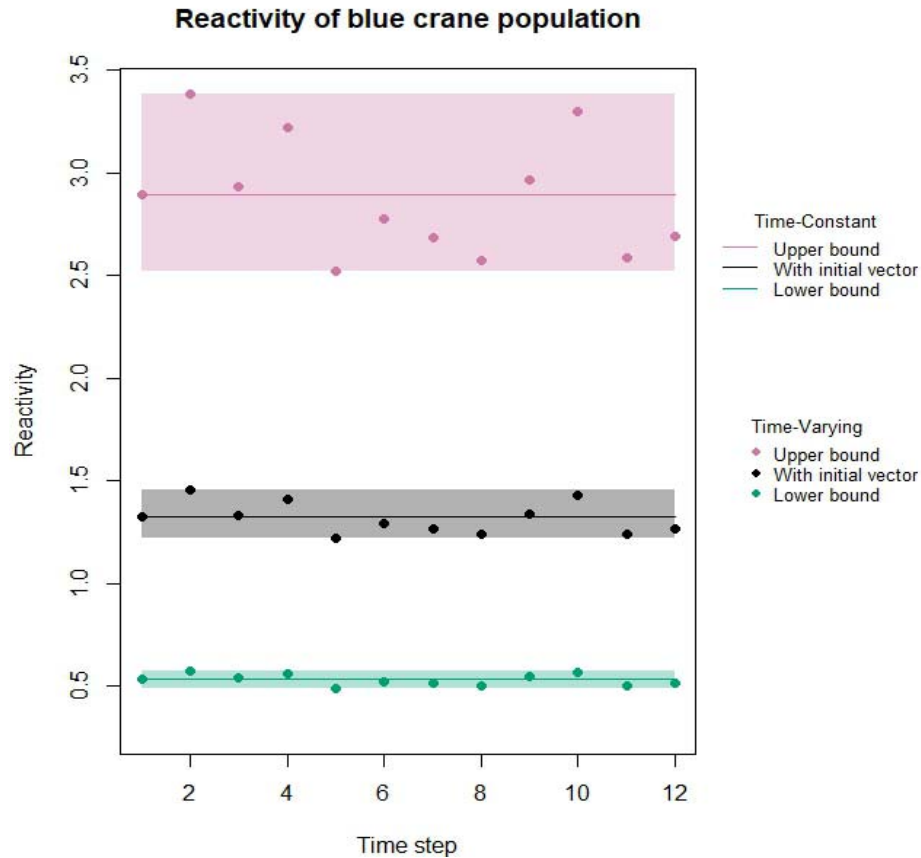
318 shown as: reac_lwr and reac_upr (for lower and upper bound, respectively). This table is the

319 output produced by the function resilience.

320

Time-step	Population name	reac_TV	reac_lwr_TV	reac_upr_TV	reac_TC	reac_lwr_TC	reac_upr_TC
1	blue crane	1.31	0.53	2.89	1.31	0.53	2.89
2	blue crane	1.44	0.57	3.38	1.31	0.53	2.89
3	blue crane	1.32	0.54	2.93	1.31	0.53	2.89
4	blue crane	1.40	0.56	3.22	1.31	0.53	2.89
5	blue crane	1.22	0.49	2.52	1.31	0.53	2.89
6	blue crane	1.28	0.52	2.78	1.31	0.53	2.89
7	blue crane	1.26	0.52	2.68	1.31	0.53	2.89
8	blue crane	1.23	0.50	2.58	1.31	0.53	2.89
9	blue crane	1.33	0.55	2.96	1.31	0.53	2.89
10	blue crane	1.42	0.57	3.30	1.31	0.53	2.89
11	blue crane	1.23	0.50	2.59	1.31	0.53	2.89
12	blue crane	1.26	0.51	2.69	1.31	0.53	2.89

321



322

323 Figure 3: Application of the function plot to visualise time-varying (dots) and time-constant
 324 (solid lines) reactivity values of the blue crane population. The reactivity is calculated with
 325 the specified initial vector and its lower and upper bounds. The shaded blocks represent the
 326 range between the minimum and the maximum of the time-varying values.

327

328 Table 3: The distance measures between the time-varying and the time-constant values of
 329 reactivity calculated for the blue crane population. This table was obtained by calling the
 330 function summary on an object returned by the function resilience.

331

Distance measures			
Resilience	RMSE	rRMSE	MAPE
metrics			
reac	0.08	0.96	0.05
reac_lwr	0.03	0.96	0.04

reac_upr 0.28 0.96 0.08 332

333

334

335

336

337

338 One application of the demographic resilience approach for conservation is to investigate
339 which (st)age class affects the resilience metrics the most. For the blue crane population the
340 upper bound of reactivity is reached when only the oldest individuals (“year 5 and older”) are
341 present (see vignette). This implies that this population will grow faster than the asymptotic
342 rate (i.e. amplify) when there is an overrepresentation of such individuals. Identifying the
343 specific (st)age classes and vital rates that can have profound effects on variation in resilience
344 of the overall population is of great importance for conservation. In the case of the blue crane,
345 our findings suggest that a population reinforcement aiming at increasing the stock of “older”
346 individuals could be used to counter the negative effects of climate change.

347

348 **Conclusions**

349 The demres package provides tools to both assess time-varying demographic resilience
350 metrics and to compare time-varying and time-constant approaches visually and
351 quantitatively. Our package draws attention to the time-varying character of resilience, and
352 permits pinpointing time intervals over which the values of demographic resilience metrics
353 were extreme. We provide a flexible piece of software that can be easily used by conservation
354 biologists, population ecologists, and managers who work on long-term studies and aim at

355 assessing the resilience of the studied population. The framework we provide allows
356 comparing demographic resilience metrics in a standardised way, facilitating the comparison
357 between populations or species in comparative studies.

358

359 **References**

360 Altwegg, R., & Anderson, M. D. (2009). Rainfall in arid zones: Possible effects of climate
361 change on the population ecology of blue cranes. *Functional Ecology*, 23(5), 1014–
362 1021. <https://doi.org/10.1111/j.1365-2435.2009.01563.x>

363 Bailey, L. D., Höner, O. P., Davidian, E., Dheer, A., Radchuk, V., Walter, L. F., White, E.
364 W., & Courtiol, A. (2024). Effects of environmental change on population growth:
365 Monitoring time-varying carrying capacity in free-ranging spotted hyenas. *bioRxiv*,
366 2024.04.11.589105. <https://doi.org/10.1101/2024.04.11.589105>

367 Benhaiem, S., Marescot, L., East, M. L., Kramer-Schadt, S., Gimenez, O., Lebreton, J.-D., &
368 Hofer, H. (2018). Slow recovery from a disease epidemic in the spotted hyena, a
369 keystone social carnivore. *Communications Biology*, 1(1), 201.
370 <https://doi.org/10.1038/s42003-018-0197-1>

371 Brodie, J. F., Muntifering, J., Hearn, M., Loutit, B., Loutit, R., Brell, B., Uri-Khob, S.,
372 Leader-Williams, N., & Du Preez, P. (2011). Population recovery of black
373 rhinoceros in north-west Namibia following poaching. *Animal Conservation*, 14(4),
374 354–362. <https://doi.org/10.1111/j.1469-1795.2010.00434.x>

375 Capdevila, P., Stott, I., Beger, M., & Salguero-Gómez, R. (2020). Towards a Comparative
376 Framework of Demographic Resilience. *Trends in Ecology & Evolution*, 35(9), 776–
377 786. <https://doi.org/10.1016/j.tree.2020.05.001>

378 Capdevila, P., Stott, I., Oliveras Menor, I., Stouffer, D. B., Raimundo, R. L. G., White, H.,
379 Barbour, M., & Salguero-Gómez, R. (2021). Reconciling resilience across ecological

- 380 systems, species and subdisciplines. *Journal of Ecology*, 109(9), 3102–3113.
381 <https://doi.org/10.1111/1365-2745.13775>
- 382 Caswell, H. (2006). *Matrix Population Models*. In *Encyclopedia of Environmetrics*. John
383 Wiley & Sons, Ltd. <https://doi.org/10.1002/9780470057339.vam006m>
- 384 Enright, N. J., Franco, M., & Silvertown, J. (1995). Comparing plant life histories using
385 elasticity analysis: The importance of life span and the number of life-cycle stages.
386 *Oecologia*, 104(1), 79–84. <https://doi.org/10.1007/BF00365565>
- 387 Gerber, B. D., & Kendall, W. L. (2016). Considering transient population dynamics in the
388 conservation of slow life-history species: An application to the sandhill crane.
389 *Biological Conservation*, 200, 228–239. <https://doi.org/10.1016/j.biocon.2016.06.014>
- 390 Gilbert, S. L., Hundertmark, K. J., Lindberg, M. S., Person, D. K., & Boyce, M. S. (2020).
391 The Importance of Environmental Variability and Transient Population Dynamics for
392 a Northern Ungulate. *Frontiers in Ecology and Evolution*, 8, 531027.
393 <https://doi.org/10.3389/fevo.2020.531027>
- 394 Hodson, T. O. (2022). Root-mean-square error (RMSE) or mean absolute error (MAE):
395 When to use them or not. *Geoscientific Model Development*, 15(14), 5481–5487.
396 <https://doi.org/10.5194/gmd-15-5481-2022>
- 397 IUCN. 2024. *The IUCN Red List of Threatened Species*. Version 2024-2.
398 <https://www.iucnredlist.org>. Accessed on [14 November 2024].
- 399 Jenouvrier, S., Aubry, L., Van Daalen, S., Barbraud, C., Weimerskirch, H., & Caswell, H.
400 (2022). When the going gets tough, the tough get going: Effect of extreme climate on
401 an Antarctic seabird's life history. *Ecology Letters*, 25(10), 2120–2131.
402 <https://doi.org/10.1111/ele.14076>
- 403 Jones, O. R., Barks, P., Stott, I., James, T. D., Levin, S., Petry, W. K., Capdevila, P.,
404 CheCastaldo, J., Jackson, J., Römer, G., Schuette, C., Thomas, C. C., &

- 405 Salguero-Gómez, R. (2022). Rcompadre and Rage—Two R packages to facilitate the
406 use of the COMPADRE and COMADRE databases and calculation of life-history
407 traits from matrix population models. *Methods in Ecology and Evolution*, 13(4), 770–
408 781. <https://doi.org/10.1111/2041-210X.13792>
- 409 Jonzén, N., Pople, T., Knape, J., & Sköld, M. (2010). Stochastic demography and population
410 dynamics in the red kangaroo *Macropus rufus*. *Journal of Animal Ecology*, 79(1),
411 109–116. <https://doi.org/10.1111/j.1365-2656.2009.01601.x>
- 412 Koons, D. N., Grand, J. B., Zinner, B., & Rockwell, R. F. (2005). Transient population
413 dynamics: Relations to life history and initial population state. *Ecological Modelling*,
414 185(2–4), 283–297. <https://doi.org/10.1016/j.ecolmodel.2004.12.011>
- 415 Marescot, L., Benhaim, S., Gimenez, O., Hofer, H., Lebreton, J., Olarte-Castillo, X. A.,
416 Kramer-Schadt, S., & East, M. L. (2018). Social status mediates the fitness costs of
417 infection with canine distemper virus in Serengeti spotted hyenas. *Functional*
418 *Ecology*, 32(5), 1237–1250. <https://doi.org/10.1111/1365-2435.13059>
- 419 Salguero-Gómez, R., Jones, O. R., Archer, C. R., Bein, C., De Buhr, H., Farack, C.,
420 Gottschalk, F., Hartmann, A., Henning, A., Hoppe, G., Römer, G., Ruoff, T.,
421 Sommer, V., Wille, J., Voigt, J., Zeh, S., Vieregg, D., Buckley, Y. M., Che-Castaldo,
422 J., ... Vaupel, J. W. (2016). COMADRE: A global data base of animal demography.
423 *Journal of Animal Ecology*, 85(2), 371–384. <https://doi.org/10.1111/1365-2656.12482>
- 424 Stott, I., Hodgson, D. J., & Townley, S. (2012). popdemo: An R package for population
425 demography using projection matrix analysis. *Methods in Ecology and Evolution*,
426 3(5), 797–802. <https://doi.org/10.1111/j.2041-210X.2012.00222.x>
- 427 Stott, I., Townley, S., & Hodgson, D. J. (2011). A framework for studying transient dynamics
428 of population projection matrix models. *Ecology Letters*, 14(9), 959–970.
429 <https://doi.org/10.1111/j.1461-0248.2011.01659.x>

- 430 Townley, S., & Hodgson, D. J. (2008). Erratum et addendum: Transient amplification and
431 attenuation in stage-structured population dynamics. *Journal of Applied Ecology*,
432 45(6), 1836–1839. <https://doi.org/10.1111/j.1365-2664.2008.01562.x>
- 433 Turner, M. G. (2010). Disturbance and landscape dynamics in a changing world. *Ecology*,
434 91(10), 2833–2849. <https://doi.org/10.1890/10-0097.1>
- 435